LUPINE PUBLISHERS

Modern Approaches on Material Science

DOI: 10.32474/MAMS.2019.02.000131

ISSN: 2641-6921

Review Article

Synergetic Reinforcement of Cu-11.0 wt.% Al Alloy with Al_2O_3 Nano-Sized Particles and Carbon Nanotubes CNTs

Eid EA* and Ragab M

Basic Science Department, Higher Technological Institute, Egypt

***Corresponding author:** Eid EA, Basic Science Department, Higher Technological Institute, Egypt

Received: September 23, 2019 **Published:** October 17, 2019

Abstract

The present research has been reinforced the aluminum bronze matrix composites (ABMCs) of weight concentration (Cu_{89}-Al_{11}) by individual and/or hybrid additions of Al_2O_3 and CNTs. ABMCs were fabricated via powder metallurgy technique. The physical properties such as density, electrical conductivity, thermal conductivity, hardness, and wear rate of the ABMCs alloys have been investigated. Microstructure features were discovered by utilizing SEM and EDX examination. The addition of 2 wt. % of CNTs was caused more refined grains and increased their uniform distribution otherwise adding of 2 wt. % Al_2O_3 agglomerates throughout the active grain boundaries. The hybrid addition of 1.0 wt. % of Al_2O_3 and 1.0Wt % CNTs improved the both hardness and wear resistance due to the physical synergistic reinforcement of them. Moreover, their good distribution at the grain boundary can form Zener pinning effect that restrict the grains growth of its matrix. Additionally, the addition of 2 wt.% CNTs enhanced the electrical and thermal conductivity of ABMCs because the CNTs creating new conductive paths in Aluminum bronze (AB) matrix.

Keywords: Powder metallurgy; Aluminum bronze alloy; Hardness; Electrical conductivity; Wear rate

Introduction

Copper and copper alloys have been considered as one of the best refractory materials due to their highly strength, excellent thermal characterization, prime corrosion resistance, good wear resistance, as well as their less cost [1,2]. Nowadays, Aluminum bronze alloys and their composites are operating effectively in electronic projects, automobile manufacturing and military industries [3]. However, their poor plasticity and limited hardness as well as low reliability restricted their application in many technological fields. Actually, these alloys have serious deficiency, where the microstructure is unstable and their grains coarsening with aging especially at elevated temperature [4]. Therefore, the major challenge is how to develop aluminum bronze alloys without loss their superior mechanical characteristics and optimum electrical conductivity. It is well known that, the incorporation of Nano-sized particles (NP) is reinforcing the copper alloys and augmented their mechanical properties without deterioration the other physical properties [5]. A new age of research is emerging in the field of copper matrix composites (CMCs) after production the carbon nanotubes (CNTs) [6]. Because, the CNTs molecules have own especial structure where their carbon atoms bonded together by sp^2 planner hybridization configuration. These chemical bonds have responsible to give CNTs particles the superior tensile strength, excellent thermal and electrical conductivity besides its distinctive physical properties [7,8]. Nevertheless, numerous issues still subsist such as inhomogeneous distribution of CNTs during mixing operation. Moreover, the faint wetting behavior between CNTs and CMCs are weakened the physical bonding which has negative effect on thermal stability and reduce their wear resistance [9].

To solve these problems, Kwon et al. succeeded to merge CNTs with helping of SiC which operative as mixing agent in Aluminum powder to obtain the uniform distribution, that lead to increase the hardness [10,11]. Du et al [12] reported that the mixing of Al_2O_3 NP with MMCs/CNTs can be augmented the interfacial cohesion between CNTs and MMCs due to improve the adhesion force as well as decrease the contact angle between them. Cui et al [13] confirmed the addition of 2 wt% SiC and 11.7 wt% nickel coated graphite into bronze alloy improved the tribological properties due to the synergistic effects of reinforcements. Moreover, they demonstrated that, the presence of Al_2O_3 improved the hardness and wear resistance of silver-bronze composites and their friction

coefficient increased with the increase of alumina [14]. Other approach has been achieved to form a hybrid synthesis of TiC and graphite particles in order to reinforce the CMCs by utilizing the microwave sintering [15]. Further, a considerable decrementing in electrical conductivity and density was observed gained by adding 15 wt% CNTs into Cu-Ti composite as reported in Ref. [4]. Also, Koppad et al revealed that the physical properties such as thermal and electrical conductivities after merging MWCNTs into Cu matrix have been reduced [16]. Unfortunately, there are little researches which discussed the effect of additions of CNTs and Al_2O_3 NP on the physical characteristics of ABMCs. Therefore, systematic research has been directed on reinforcement the Cu-11wt% Al alloy by different additives of single and/or hybrid concentrations of nano-sized Al_2O_3 particles and Multi-wall carbon nano-tubes (CNTs). Furthermore, the powder metallurgy technique has been utilized for incorporating the desirable nano-particles to attain the best physical and mechanical properties. In addition, the fabricated specimens were researched to reveal their different physical properties like mechanical and electrical characteristics.

Experimental work

Raw Materials

Table 1: The characteristic of materials are used in this research.

Materials	Shape	Size	Purity %	Source of materials
Copper	Powder	70 mm	99.8	Alpha Chemika, Co.
Aluminum	Powder	100 mm	99.8	Alpha Chemika, Co.
Al_2O_3	Nano-size powder	50 nm	99.99	Sigma Aldrich, Co.
MWCNTs	Nano-size dust	D0 ≈ 25 L ≈ 35 mm	95	Nanotech Egypt Co.

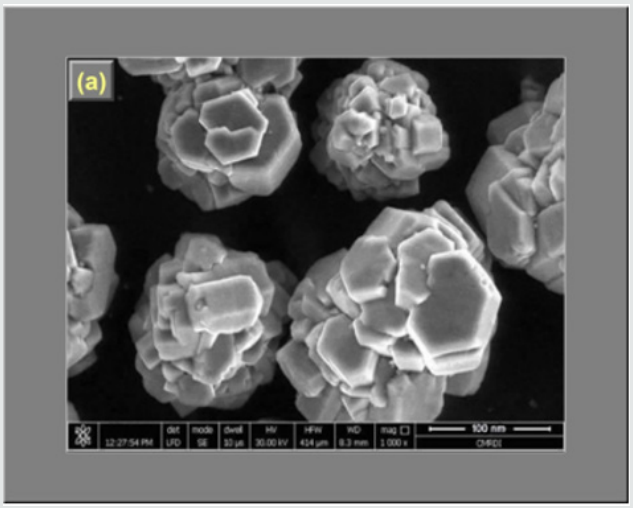

Figure 1(a): FE-SEM image of Al_2O_3 nano-sized particles.

Powder of Copper (Cu) and Aluminum (Al) were utilized as basic material to fabricate the aluminum bronze matrix composites (ABMCs). In addition, the ABMCs were loaded by CNTs and Al_2O_3 nano-sized particles as reinforcement substances. The characteristic of the starting materials that were employed to prepare the tested alloys were listed in Table 1. Additionally, (Figures 1a-b) shows FE-SEM image and X-ray diffraction pattern of Al_2O_3 nano sized particles.

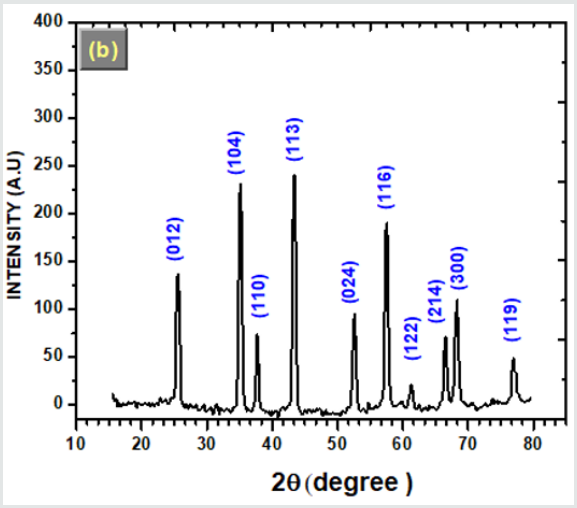

Figure 1(b): XRD pattern of Al_2O_3 NP.

Purification of CNTs

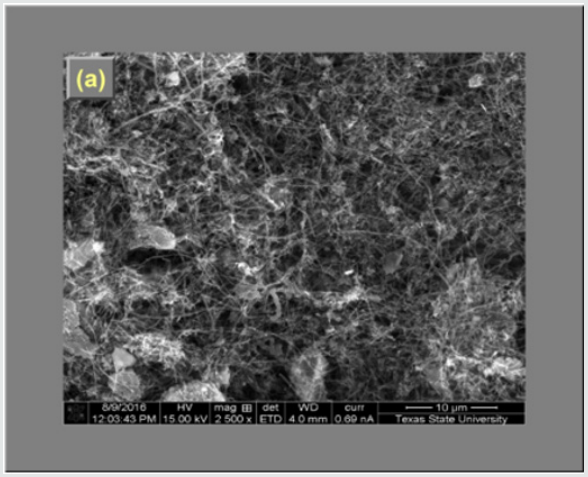

Figure 2(a): SEM image of purified CNTs.

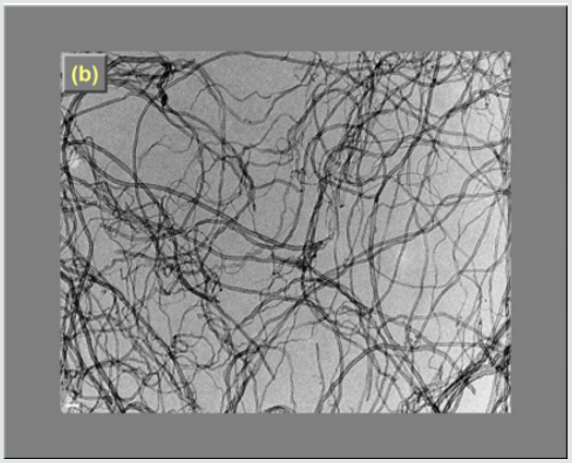

Figure 2(b): TEM image of purified CNTs.

In the beginning, the CNTs were refined by ultrasonic shaking them in warm water bath containing acidic aqueous solution of (3:1) H_2SO_4/HNO_3 at 60°C for time of 3hr. Then the purify CNTs were washed and have filtered with distilled water until chemically neutralized (pH=7.0) and were dried in electric furnace at 50°C. (Figure 2a-b) exhibits the SEM and TEM images of carbon nanotubes (CNTs) after purification.

Powder Metallurgy Fabrication of ABMCs

A. Blending

The initial powders of Cu and Al metals were blended in a weight ratio of 89 Cu: 11 Al by ball milling machine for 90 min at 300 rpm. The anhydrous 2.0 wt % of acetone was used as binder medium. The mixing process was performed in stainless steel pot containing several small stainless-steel balls (Φ=10 mm). Then, the obtaining composite powders of Cu-11wt. % Al were placed in dryer for 60 min at 80 °C to evaporate the acetone. The similar steps were employed to prepare the composite powder that loaded by CNTs and/or Al_2O_3 NP. Four specimens were equipped by their weight as following; 89 wt.% Cu-11 wt.% Al matrix alloy (abbreviated as AB), 87 wt.% Cu - 11 wt.% Al - 2.0 wt.% CNTs (abbreviated as AB/CNT), 87 wt.% Cu - 11 wt.% Al- 2.0 wt.% Al_2O_3 (abbreviated as AB/Al_2O_3) and 87 wt.% Cu -11 wt.% Al-1.0 wt. % CNTs -1.0 wt.% Al_2O_3 (abbreviated as AB/CNT/Al_2O_3).These constituent of powder composites alloys were recorded in Table 2.

Table 2: Chemical composition and concentration (weight %) of studied composite alloys.

Alloys	Abbreviation	Cu	Al	Al_2O_3	CNTs
Cu-11.0 wt% Al	AB	89.00	11.00	--	--
Cu-11.0 Al-2.0 wt% Al_2O_3	AB/Al_2O_3	87.00	11.00	2.00	--
Cu-11.0 Al-2.0 wt% CNTs	AB/CNTs	87.00	11.00	--	2.00
Cu-11.0 Al-1.0 Al_2O_3-1.0 wt% CNTs	AB/Al_2O_3/CNTs	87.00	11.00	1.00	1.00

B. Compacting

In this search, powder metallurgy method was utilized to acquire the desired composite specimens. It is worth to note that, many researchers have notified a mixing of Cu powder with CNTs is a great challenge, since they are easily detached from each other. Therefore, this research suggested to an efficient method to obtain a good mixture by employing a chemical factor as cyclohyxane (C_6H_{12}) with paraffin wax as a lubricant material to lower friction and create appropriate medium to perform the mix process between CNT with the Cu/Al powder [17]. The preparing blended powder of plain alloy and their composites were loaded gradually into steel die of a cavity cylinder its inner diameter is ~ 8.0 mm and its height~50.0 mm. The blended powder of specimens compacted at pressure of 800 MPa for 90 min by utilizing the hydraulic uniaxial pressing machine modified with high power heater.

C. Sintering

Sintering is the final operation to form a solid phase of ABMCs by heating and/or pressuring the specimens at temperature lower than the melting point of Cu/Al matrix. The atoms of constituent substance were diffused across the boundaries of the agglomeration particles and fuse the particles together and create one solid piece. Therefore, sintering specimens gain good internal strength and have better properties. The sintering process of virgin specimens was carried out in vacuum muffle furnace at 900°C for 1.5 hours with heating rate of 10°C/min and cooled at rate of 20°C/min, and then the specimens have gradually cooled to ambient temperature and obtain the specimens as cylindrical rods of 8 mm diameter. Furthermore, (Figure 3) summarized the graphical abstract for preparing steps and different processing that carried out to obtain the desired alloys.

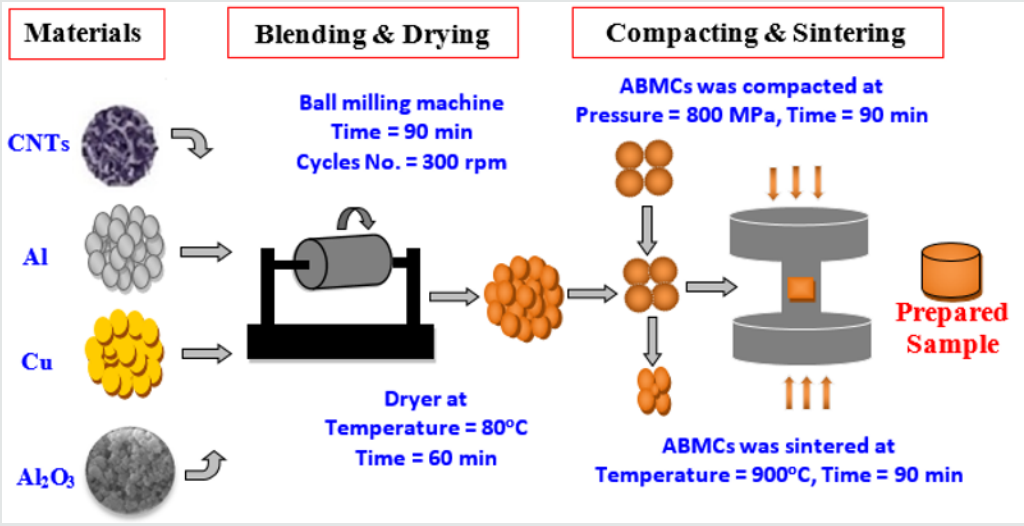

Figure 3: Graphical abstract of powder metallurgy steps for processing the investigated ABMCs.

Characterization and Measurements;

To examine the microstructural features, thick discs of samples were equipped for polishing via employing a different sizes of emery papers from Silicon carbide (from 120 to 3000), then shinned by using micronized of diamond paste. The microstructural characteristics as well as the distribution of the different phases were investigated utilizing the field emission scanning electron microscopy (FE-SEM; SEM-JEOL JSM5800-LV). This apparatus was equipped with a unit of an energy dispersive X-ray spectrometry (EDX) to detect the chemical configuration of the observed different phases. The floating Archimedes principle was used to determine the actual density $(\rho_{act.})$ of the sintered samples according to the following equations [17,18]:

$$(\rho_{act.}) = W_{air} / (W_{air} - W_{water}) \quad (1)$$

Where W_{air} and W_{water} are weight of the specimen in air and pure liquid of toluene, respectively, Vickers hardness measurement was carried out at a load of 1.0 kg throughout time 15 seconds. Lecco Vickers hardness analyzer, Model: LV 700, USA, was used to evaluate average value of hardness of tested composite alloys. (Average of seven readings at different position was taken for each alloy).

Pin-on-disk technique was employed to measure the wear behavior of ABMCs alloys. Wire cut machine was used to obtain the cylindrical shaped specimens of 5 mm in diameter from the tested composites alloys. Moreover, according to ASTM G99 standards for dry sliding wear test, the flat polished contact area (≈ 12.57 mm^2) of cylindrical sample was prepared. The wear tests were performed at different nominal load 2, 4, 6 N with sliding speed 1.5 m/s which equivalent to angular speed 250 rpm and the contact length of sliding was kept consistent at 1000 m for each composite alloy. The mass of the sample was gauged before and after the test with highly accuracy electronic balance (0.0001g) to calculate the weight loss. Moreover, to obtain the accurate result of wear loss every individual testing was performed three times and their average value was calculated, then this value was considered during the calculations of wear rate. Further, wear volume (ΔV) is calculated via Eq. (2), and the specific dry sliding wear rate (ψ) of the tested alloys is evaluated via Eq. (3) [19].

$$\Delta V = \frac{Weight\ loss}{density} \quad (2)$$

$$\Psi = \frac{\Delta V}{p \times d} \quad (3)$$

Where (*P*) and (*d*) is applied normal load (N) on pin and the sliding distance (m), respectively. The electrical resistivity and/or electric conductivity of tested alloys was measured by Motwane Digital Micro ohm meter (LR-2045) which is capable of measuring very low resistance in micro ohm as low as 0.1 μΩ. Then, the electric conductivity (**σ**) is dependent on resistance (R) of the specimen that was evaluated using the following formula [18,20].

$$\sigma = \frac{L}{A \times R} \quad (4)$$

Where L and A are the length between the ohmmeter terminals and area of measured sample, respectively. Furthermore, thermal conductivity (**K**) can be calculated theoretically via the value of (**σ**) by utilizing the Wiedemann-Franz formula [17,18]

$$K = \alpha \sigma T \quad (5)$$

Where α is Lorenz number (2.45 x10^{-8} W/Ω.k^2) and **T** is temperature in Kelvin.

Results and Discussion

Microstructure Features

The study of microstructure evolution and understanding of the material phases are very important for increase the scientific knowledge and technological progress. Therefore, in this section the microstructural characteristics of ABMCs were described and discussed. (Figure 4a-b) exhibits SEM images and EDX elemental analysis of different motifs in sintering monolithic AB alloy. EDX analysis in Figure 3b confirms that light gray regions are Al phase and dark grey is considered as Cu phase. SEM image of the monolithic AB alloy in Figure 3a has revealed a little void result to the mutual uniform distribution of both elements. Moreover, grain size of Al phase is smaller than that Cu phase which lead to permit them to occupy or fill the empty spaces between Cu grains. The higher affinity between Cu and Al at temperature greater than 120°C is main reason for forming several sorts of intermetallic compounds (IMCs). However, according to Cu-Al phase diagram which confirmed five kinds of IMCs (Al_2Cu, AlCu, Al_3Cu_4, Al_2Cu_3 and Al_4Cu_9) are formed in temperature range 350-500°C [2]. Otherwise, microstructural examinations for all ABMCs alloys have cleared that, there is no IMCs was created in their matrices. (Figure 5a) exhibits that the adding of 2.0 wt. % Al_2O_3 nanoparticles has great effect on morphology and grains distribution of AB/Al_2O_3 alloy. Thence, approximately small grains and nearly homogeneity texture as well as little voids were observed. Furthermore, agglomerated shapes were appeared along the coarse grain boundaries. EDX elementals analysis in Figure 5b confirms that white dots embedded in AB matrix are Al_2O_3 agglomerated particles.

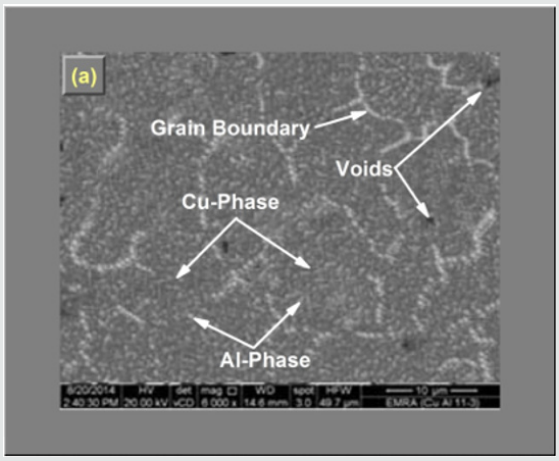

Figure 4(a): SEM image of AB alloy.

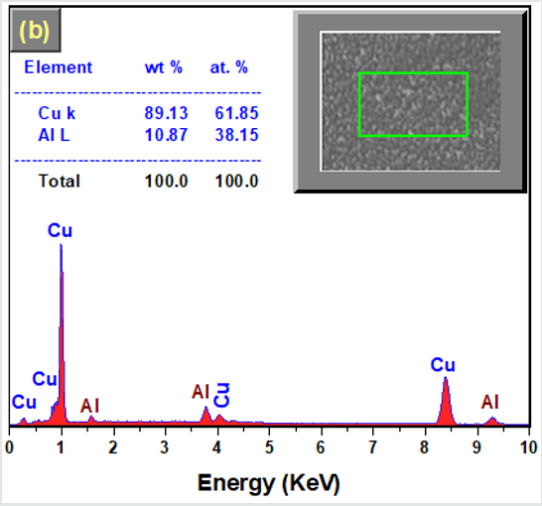

Figure 4(b): EDX analysis and its elemental configuration of white and gray regions.

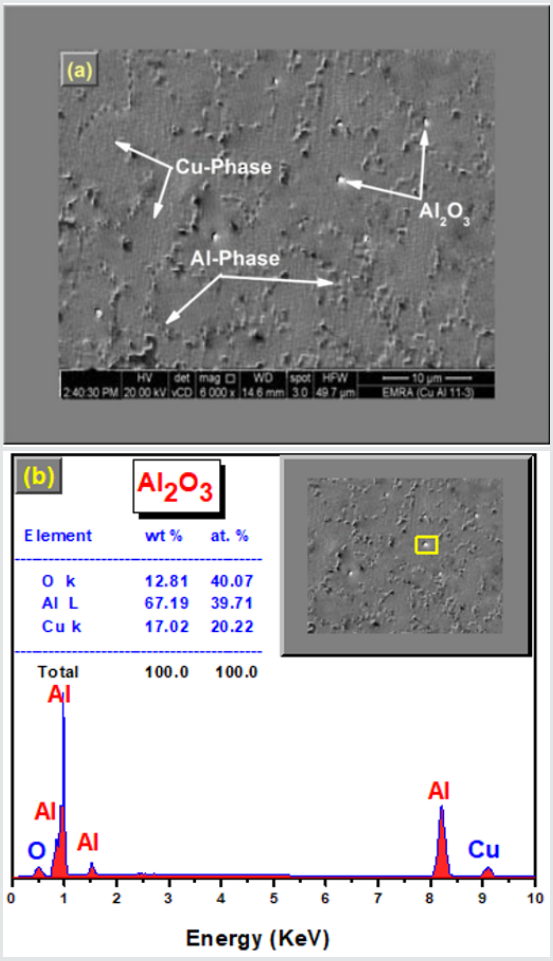

Figure 5(a-b): (a) SEM image of AB/Al_2O_3 composite alloy and (b) EDX analysis the elemental configuration of white dots.

Moreover, the (Figure 6a) depicts the microstructure of AB/CNTs alloy. It is clear that the addition of 2 wt. % of CNTs into AB alloy matrix causes more refined grains and increases their uniform distribution. This can be attributed to the ability of Al to motivate the bonding creation between CNTs and Cu phase that play an important factor for improving the physical and mechanical characteristics [12,20]. Additionally, (Figure 6b) reveals the EDX elemental analysis of very dark black region that appear in SEM micrograph of sintered AB/CNTs alloy. The elemental analyses were confirming that 23.8 at. % of carbon phase associated with 66.61 at. % and 8.1 at. % of copper and aluminum phase, respectively. This analysis indicated that CNTs covered and restricted the growth of AB grains which explain the reduction of their grain size. On other hand, the dual addition of 1 wt% Al_2O_3 and 1 wt% CNTs with AB alloy causes great positive evolution on the microstructure texture of AB/Al_2O_3/CNTs hybrid alloy as revealed in (Figure 7a). Notably, the hybrid composite alloy has gathered the benefits of both additions of Al_2O_3 and CNTs. Thence; the hybrid alloy has an excellent homogenous distribution plus fine edge grain boundary as well as the intrinsic voids nearly absent. In addition, some micro size agglomerations of Al_2O_3 and CNTs appeared within grains and/or at triple joint between grain boundaries this due to the good mixing process between Cu, Al and the additives during blending and sintering process. Further, the (Figure 7b-c) exhibits the EDX elemental analysis of different phases that have existed in SEM micrograph of hybrid composite alloy.

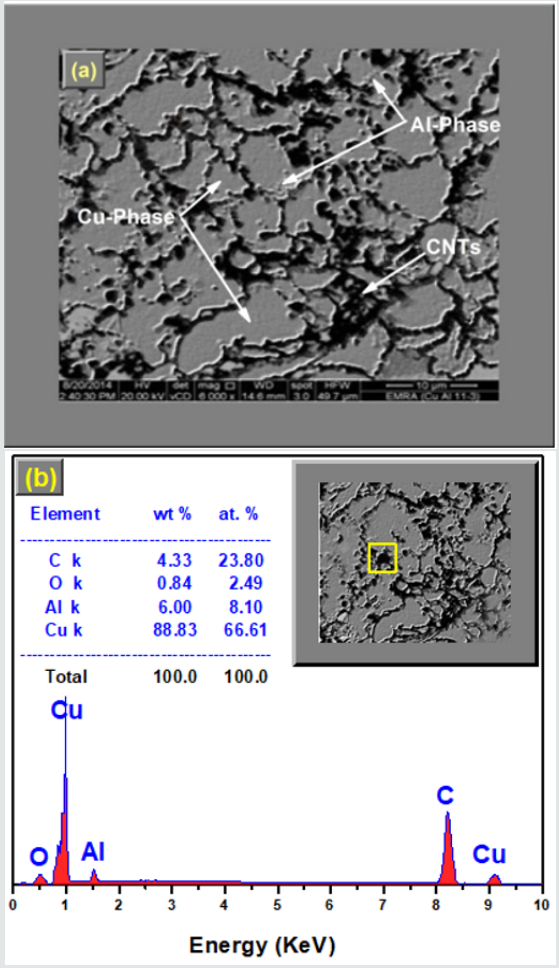

Figure 6(a-b): (a) SEM image of AB/CNTs alloy and (b) EDX analysis and elemental configuration of dark motifs.

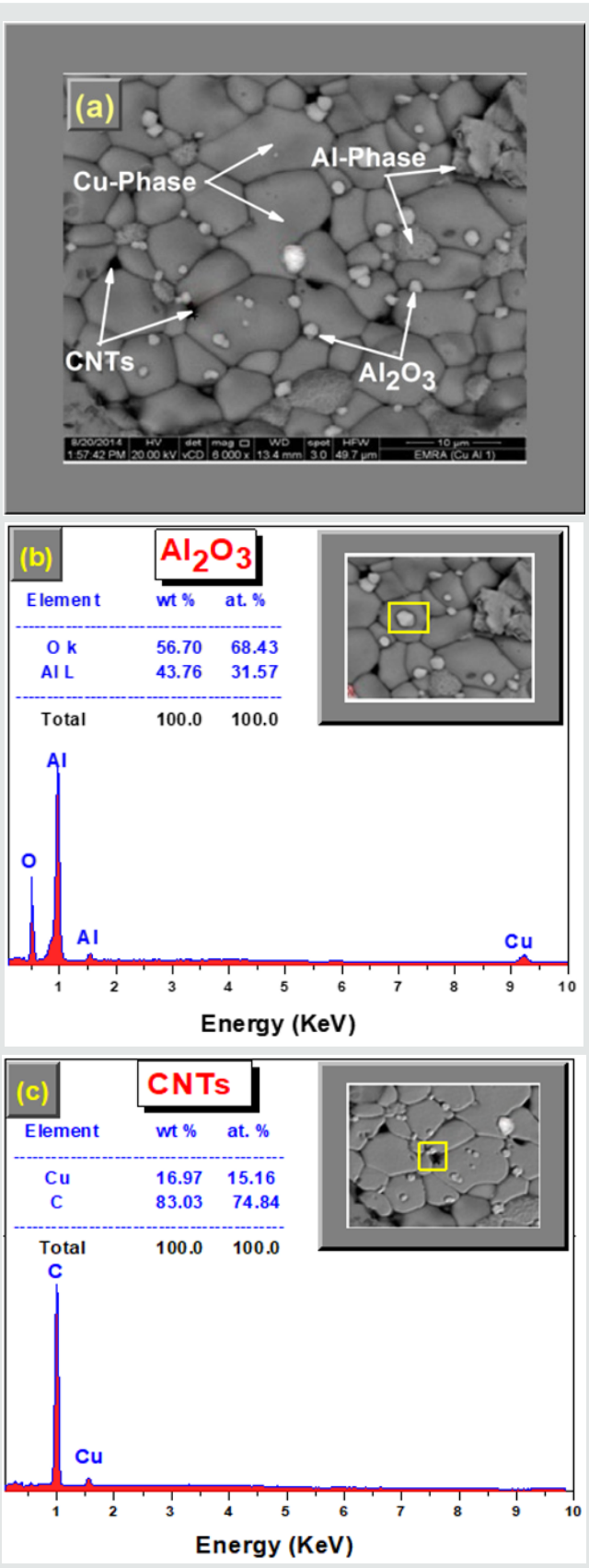

Figure 7(a-c): (a) SEM image of AB/Al2O3/CNTs hybrid composite alloy and (b) EDX analysis and its elemental configuration of Al_2O_3 nanoparticles (c) EDX analysis and its elemental configuration of CNTs.

The Experimental and Theoretical Density

The essential factor of equipped alloys by powder metallurgy is the apparent density that influence on its physical and mechanical characteristics. Figure 8 shows the actual density ($\rho_{act.}$) of monolithic AB alloy and their composites that contain various kinds of reinforcement ingredients. The results have indicated that the values of experimental and theoretical density ($\rho_{ther.}$) are nearly closed to each other. Furthermore, the relative density of AB /CNTs composite alloy has slightly decreased than monolithic alloy and /or other composite alloys. Additionally, the apparent density of hybrid composite alloy was increased than that containing an individual addition of Al_2O_3 nanoparticles or CNTs. These results can be explained based on the difference values of thermal expansion coefficient (CTE) between AB matrix, CNTs and Al_2O_3 nanoparticles. On other hand, the large difference between the density of AB Matrix (7.56 g/cm^3) and their additives (density of Al_2O_3 = 3.98 g/cm^3 and CNTs = 1.8 g/cm^3) lead to decrease the apparent density of the composite alloys [20]. On other hand, the increase in density of hybrid metallic composite alloy (AB/Al_2O_3/CNTs) can be correlated to the merge of minor amounts of CNTs gives a uniform dispersion as well as the addition of Al_2O_3 resulting to improve its density due to fill up the intrinsic voids.

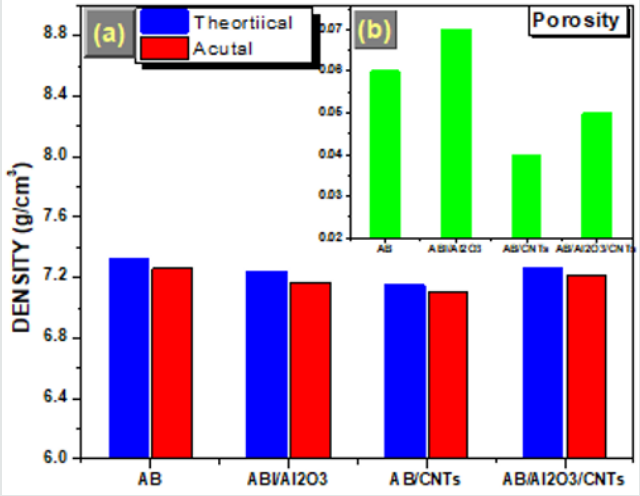

Figure 8a-b: (a) The actual and theoretical density and (b) calculated porosity of different ABMCs alloys.

Microhardness

Hardness test is widely employed in laboratory and industrial field as a fast and inexpensive test to obtain the value of deformation resistance for different materials. The hardness value of a metal helps to design the static mechanical properties. The microhardness of the investigated composite alloys was measured by Vickers microhardness tester and their results are depicted in Figure 9. The results of the hardness indicated that AB/Al_2O_3 as well as AB/CNTs alloy has a higher hardness than monolithic AB alloy. On other hand, the Al_2O_3 nanoparticles addition has more effective hardening than the addition of CNTs. Thence, the CNTs has low bonding behavior

with AB matrix due to its poor wetting with Cu element as well as its large surface area inhibit the motion of Cu or Al atoms during sintering process [18,20]. Generally, the augmentation of hardness after addition of Al_2O_3 nanoparticles and/or CNTs can be attributed to synergetic reinforced nature of nanoparticles as well as their pinning effect on the grain boundaries of AB matrix. Furthermore, the increase in hardness that observed after additions of CNTs and/or Al_2O_3 can be correlated to the strengthening effect of them. Since, the mechanical properties of CMCs are dependent on several factors such as

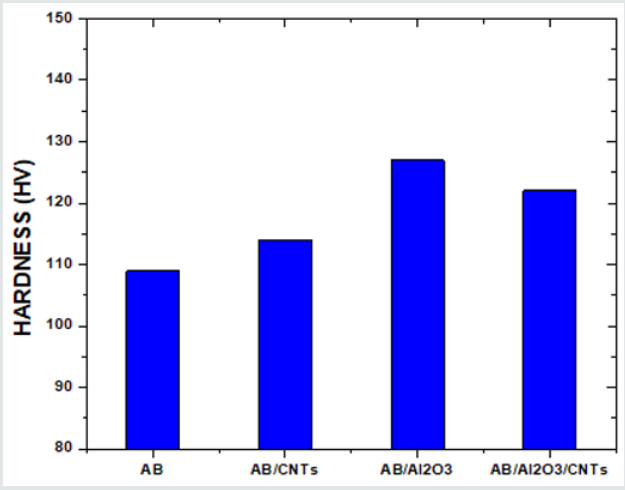

Figure 9: The hardness values of different ABMCs alloys.

(i) Physical and chemical nature of reinforcement particles,

(ii) Dislocation density and their distribution, and

(iii) Grain size plus their uniform distribution.

Additionally, the thermal mismatch between different ingredients of CMCs leads to create strain fields which hump the mobility of dislocation and strengthens the CMCs matrix [21]. Thus, based on the rule of strengthening metallic mixtures and the higher hardness values of our additives (CNTs and Al_2O_3) we can interpret the improvement of hardness values of the tested alloys.

Wear Volume and Specific Wear Rate

The wear characteristics of composite alloys were examined by measuring their wear loss and wear rate. Figure 10a shows the volume wear loss of AB, AB/Al_2O_3, AB /CNTs, and AB /CNTs/Al_2O_3 composite alloys by utilizing a dry sliding wear condition. These curves appear the difference in wear loss of AB alloy and other composite alloys against the applied load. One can observe that, under all loads AB alloy displayed higher wear loss than other metallic composite alloys. Otherwise, the AB/CNTs/Al_2O_3 hybrid composite alloy exhibited lower volume wear loss than the other composite alloys. Moreover, it is clear that volume wear loss behavior of tested composite alloys is largely influenced by applied load and kind of the nano addition. Figure 10b shows the specific wear rate of the tested composite alloys as a function of different loads. The specific wear rate was measured to be $4.03\times10^{-5}mm^3/Nm$ for monolithic AB alloy and 1.41×10^{-5} mm^3/m for AB/CNTs/Al_2O_3 hybrid composite alloy at load of 6 N. In general; the single addition of CNTs and/or Al_2O_3 nanoparticles remarkably reduced the wear rate and so improved the wear resistance of the composite alloys. It is clear that wear loss and wear rate is dramatically decreased with the addition of 2 wt. % Al_2O_3 nanoparticles and/or CNTs. This is due to presence of CNTs aggregates and nanoparticles of Al_2O_3 which are smeared the contact surface of counterparts of pen and counterpart of harden wear disk. Hence, these aggregates act as good solid lubricant that reduced the friction behavior [22]. On other hand according to the atomic bond's theory, the aggregates of CNTs and Al_2O_3 nanoparticles have hexagonal structure and its atomic bonds in basal planes are very strong covalent bond, but atomic bonds between basal planes are weak physical Van-der-Waals bond. Therefore, these weak bonds are easily broken by shearing strength during dry sliding wear and cause the decrement in the value of friction coefficient and/or wear rate [23]. Furthermore, the reduction in wear rate is correlated with augmentation of hardness according to Archard rule of sliding wear that is given by the following equation [24].

$$\Delta V = K\frac{PL}{H}$$

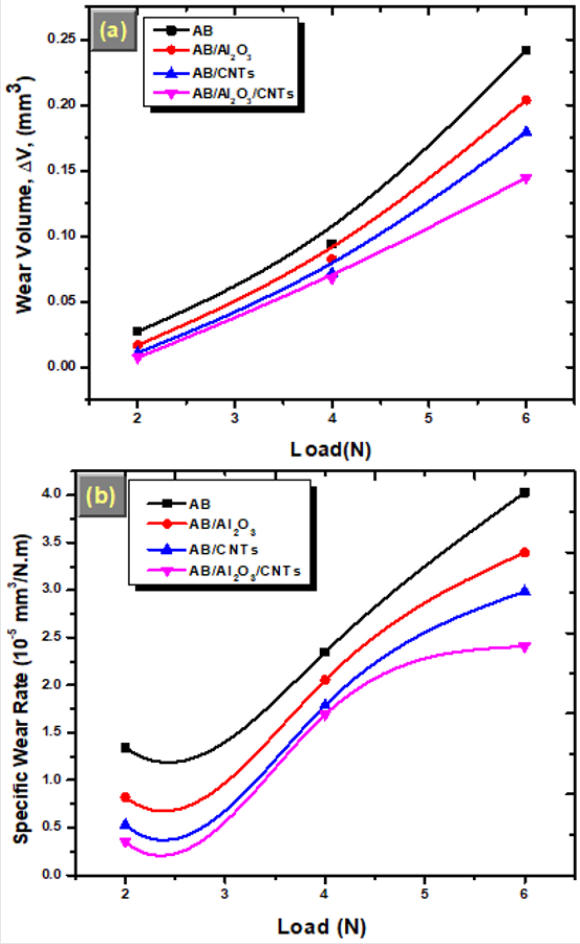

Figure 10(a-b): (a)The wear volume of different ABMCs alloys at different loads, (b) The specific wear rate of different ABMCs alloys at different loads.

Where (ΔV) is loss volume during sliding wear distance (L) under applied normal load (P), K and H are dimensionless wear coefficient and hardness of material, respectively. Generally, the wear resistance $\left(R_w = \frac{H}{K}\right)$ of material is direct proportional with its hardness.

Electrical and Thermal Conductivity

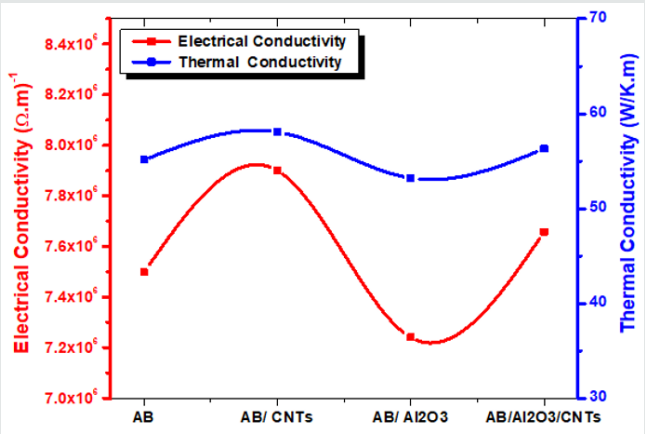

Figure 11: The electrical and thermal conductivity of ABMCs alloys at room temperature (27˚C).

Figure 11 illustrates the electrical conductivity of the tested ABMCs alloys at room temperature (T = 23°C); the AB/Al_2O_3 matrix has showed the lowest electrical conductivity (σ) comparing to other alloys. This slightly decrease in (σ) can be related to the intrinsic properties of Al_2O_3 nanoparticles which has a low electrical conductivity [20]. Otherwise, AB/CNTs have exhibited highest electrical conductivity due to existence the conductive CNTs particles which create new conducting paths between Cu and Al phases. This increase may be due to unzipping the carbon tubes or partial fragmentation which takes places during the metallurgical processes of preparation at high temperatures. This exfoliation is resulting to the creation of nano carbon sheets which are considered as a perfect electrical and thermal conductor [8]. Moreover, the electric conductivity of AB/CNTs/Al_2O_3 alloy is nearly similar to the monolithic AB alloy but slightly decrease than AB/CNTs alloy. This decrement is due to Al_2O_3 nanoparticles is considered as center scattering for the charge carriers that lead to shortness the mean free paths of movable electrons. Furthermore, the thermal conductivity (K) of the investigated AB matrix and their metallic composites is exhibited in Figure 11. It is calculated based on the empirical equation as mentioned in section of experimental measurements. In general, the behavior of their thermal conductivity is dependent on the ingredient addition and the change in their values is simple various. Notably, the AB/Al_2O_3 metallic composite alloy has revealed lower (K) value comparing to that of other metallic composites. This decrement in (K) can be correlated to the lower thermal conductivity of Al_2O_3 nanoparticles addition which is considered as insulating material (≈ 30 W/m.K). Additionally, Cu-Al/CNTs have displayed highest (K) due highly thermal conductivity of CNTs (≈ 6 ×103 W/m.K) [8,17].

Conclusion

In summary, the ABMCs reinforced by signal and/or hybrid additions of Al_2O_3 and CNTs were fabricated through powder metallurgy technique. Microstructure features were discovered by utilizing SEM and EDX examination. SEM image of the monolithic AB alloy contain a little void due to mutual uniform distribution of both elements and Al entities are occupied the empty spaces in Cu phase. The addition of 2 wt. % of CNTs causes more refined grains and increases their uniform distribution otherwise adding of Al_2O_3 NP agglomerates along the coarse grain boundaries. Furthermore, the dual addition of Al_2O_3 and CNTs has great positive effect on microstructure texture and other properties of hybrid alloy. The density of AB/CNTs composite alloy has slightly decreased than monolithic AB alloy and other composite alloys due to the large difference between the density of their constituents and density of CNTs. This research demonstrates the Archard rule of simultaneous enhancement of hardness and wear rate in hybrid composite alloy, which are attributed to the synergistic reinforcement of CNTs and Al_2O_3 nanoparticles. Hence, The Al_2O_3 can act as an active mixing agent to improve the dispersion of CNTs during blending process. Furthermore, the Al_2O_3 and CNTs distributing at the grain boundary can form a Zener pinning effect to restrain the grain growth of composites. On other hand the single addition of CNTs has exhibited the highest electrical and thermal conductivity comparing to other AB composites alloys because the CNTs create new conducting paths in AB matrix. Furthermore, during the metallurgical processes may be occurring the unzipping of CNTs and creating nano carbon sheets which are considered as a perfect electrical conductor. Therefore, this study may shed some light on understanding the strengthening mechanisms and guide the rational interface design for fabricating ABMCs with high strength and good wear rate without decreasing the electrical conductivity.

References

1. Roger Francis (2010) The Corrosion of Copper and Its Alloys: A Practical Guide for Engineers. The Corrosion Society, pp. 8-11.
2. Davis JR (2001) Copper and Copper Alloys. ASM International.
3. Eswara Prasad N and Wanhill RJH Aerospace Materials and Material Technologies. Aerospace Materials, ISSN 2509-6400, ISSN 2509-6419 (electronic) Indian Institute of Metals Series ISBN 978-981-10-2133-6 ISBN 978-981-10-2134-3 1: 247-251.
4. Chu K, Chang Jia C, Sheng Li W, and Wang P (2013) Mechanical and electrical properties of carbon-nanotube-reinforced Cu-Ti alloy matrix composites. Phys. Status Solidi A210 3: 594-599.
5. Paulo Davim J (2014) Metal Matrix Composites. ISSN 2192-8983, ISBN 978-3-11-031541-7, e-ISBN (PDF) 978-3-11-031544-8 Walter de Gruyter GmbH, Berlin/Munich/Boston.
6. Singh A, Prabhu TR, Sanjay AR, Koti V (2017) An overview of processing and properties of Cu/CNT nano composites. Materials Today: Proceedings 4: 3872-3881.

7. Geim AK, Philip K (2008) Carbon wonderland. Scientific American 298(4): 90-97.
8. Popov VN (2004) Carbon nanotubes: properties and application. Materials Science and Engineering 43(3): 61-102.
9. Qiao Y, Cai X, Zhou L, Pan W, Yang C, et al. (2018) Microstructure and mechanical properties of copper matrix composites synergistically reinforced by Al_2O_3 and CNTs. Integrated Ferroelectrics 191: 133-144.
10. Kwon H, Saarna M, Yoon S, Weidenkaff A, Leparoux M (2014) Effect of milling time on dual-nanoparticulate-reinforced aluminum alloy matrix composite materials. Material Science and Engineering A 590: 338-345.
11. Kwon H, Cho S, Leparoux M, Kawasaki (2012) A Dual-nanoparticulate-reinforced aluminum matrix composite materials. Nanotechnology 23: 1-9.
12. Du ZL, Tan MJ, Guo JF, Bi GJ, Wei J (2016) Fabrication of a new Al-Al_2O_3-CNTs composite using friction stir processing (FSP). Material Science and Engineering A 667:125-131.
13. Cui G, Bi Q, Niu M, Yang J, Liu W (2013) The tribological properties of bronze-SiC-graphite composites under sea water condition. Tribology International 60: 25-35.
14. Cui G, Bi Q, Yang J, Liu W (2013) Fabrication and study on tribological characteristics of bronze-alumina-silver composite under sea water condition. Materials and Design 46: 473-484.
15. Chandrakanth GR, Rajkumar K and Aravindan S (2010) Fabrication of copper TiC-graphite hybrid metal matrix composites through microwave processing. Int J Adv Manuf Technol 48: 645-653.
16. Koppad PG, Rama HRA, Ramesh CS, Kashya KT, and Koppad RG (2013) On Thermal and Electrical Properties of Multiwalled Carbon Nanotubes/ Copper Matrix Nanocomposites. Journal of Alloys and Compounds 580: 527-532.
17. El-Khatib S, Shash AY, Elsayed AH and El-Habak A (2017) Effect of carbon nano-tubes and nano dispersion of SiC and Al_2O_3 on mechanical and physical properties of pure copper. Review Advance Material Science 52: 126-133.
18. El-Khatib S, Shash AY, Elsayed AH, El-Habak A (2018) Effect of carbon nano-tubes and dispersions of SiC and Al_2O_3on the mechanical and physical properties of copper-nickel alloy. Heliyon 4: 00876.
19. Sharma VK, Singh RC, Chaudhary R (2018) Experimental study of tribological behavior of casted aluminum bronze. Materials Today: Proceedings 5: 28008-28017.
20. Pan Y, Xiao S, Lu X, Zhou C, Li Y, et al. (2019) Fabrication, mechanical properties and electrical conductivity of Al2O3 reinforced Cu/CNTs composites. Journal of Alloys and Compounds 782: 1015-1023.
21. Mokdad F, Chen DL, Liu ZY, Xiao BL, Ni DR, et al. (2016) Deformation and strengthening mechanisms of a carbon nano tube reinforced aluminum composite. Carbon 104: 64-77.
22. Akbarpour MR, Alipour S, Safarzadeh A, Kim HS (2019) Wear and friction behavior of self-lubricating hybrid Cu-(SiC + x CNT) composites. Composites Part B 158: 92-101.
23. Sarmadi H, Kokabi AH, Seyed Reihani SM (2013) Friction and wear performance of copper-graphite surface composites fabricated by friction stir processing (FSP). Wear 304: 1-12.
24. Archard JF (1953) Contact and rubbing of flat surfaces. J Appl Phys 24: 981.

DOI: 10.32474/MAMS.2019.02.000131